Signatures of interfacial topological chiral modes via RKKY exchange interaction in Dirac and Weyl systems

Ganesh C. Paul [1,2,*] SK Firoz Islam [3,†] Paramita Dutta [4,‡] and Arijit Saha [1,2,§]

[1]*Institute of Physics, Sachivalaya Marg, Bhubaneswar 751005, India*
[2]*Homi Bhabha National Institute, Training School Complex, Anushakti Nagar, Mumbai 400085, India*
[3]*Department of Applied Physics, Aalto University, P.O. Box 15100, FI-00076 Aalto, Finland*
[4]*Department of Physics and Astronomy, Uppsala University, Box 516, S-751 20 Uppsala, Sweden*

We theoretically investigate the features of Ruderman-Kittel-Kasuya-Yosida (RKKY) exchange interaction between two magnetic impurities, mediated by the interfacial bound states inside a domain wall (DW). The latter separates the two regions with oppositely signed inversion symmetry broken terms in graphene and Weyl semimetal. The DW is modeled by a smooth quantum well which hosts a number of discrete bound states including a pair of gapless, metallic modes with opposite chiralities. We find clear signatures of these interfacial chiral bound states in spin response (RKKY exchange interaction) which is robust to the deformation of the quantum well.

I. INTRODUCTION

The emergence of the gapless one-dimensional (1D) chiral modes across the interface of two nonequivalent trivial or topological insulators has received significant attention owing to its potential application as one-way wave propagation in two-dimensional (2D) honeycomb photonic lattice [1,2] as well as spin and valley selective charge transport in 2D Dirac materials [3,4]. The underlying physics lies in the sign change of the symmetry breaking parameter across the interface, forming a quantum well (QW) which acts as a domain wall (DW) separating the two insulators. The chiralities of these interfacial modes, corresponding to the two valleys of the Dirac materials, are sensitive to the types of broken symmetry. The time reversal symmetry (TRS) breaking leads to the same chirality of the interfacial modes [1], whereas they appear with opposite chirality for inversion symmetry (IS) broken systems [5–7]. Such interfacial chiral modes (ICM) have also been found in bilayer graphene [8–11] which motivated proposing a bilayer graphene based Cooper pair beam splitter with maximum efficiency [12]. Subsequently, similar investigations were carried out in silicene [3] and surfaces of three-dimensional (3D) topological insulators [13]. Very recently, a pair of ICM have been revealed in 3D spin-1 topological semimetal where TRS is broken by means of light [14].

In recent times, the intriguing topological properties of 3D Weyl semimetal (WSM) have attracted a great deal of attention in the research community [15–20]. One major focus is the IS broken WSM where the valence and conduction bands touch each other at minimum four or more topologically protected Weyl nodes [15,18,19]. These nodes are separated both in momentum and energy, and the low energy spectrum which is linear around these nodes is described by the Weyl equations. Each Weyl node of the WSM manifests definite chirality with a total of zero as it always appears in pairs in the momentum space [21]. The chirality property of the bulk band and the surface Fermi arcs lead to several exotic phenomena in WSM [22–29].

With this framework, in this article, we analytically show the emergence of ICM in IS broken WSM. Probing these ICM remains always challenging because of its geometric confinement within the DW. In the present work, we also aim to extract the direct signatures of these ICM via Ruderman-Kittel-Kasuya-Yosida (RKKY) [30–32] exchange interaction between two magnetic impurities placed across the DW created in gapped graphene and in WSM with broken IS. It is an indirect exchange interaction mediated by the conduction electrons of the host material and already investigated extensively in different Dirac materials [33–39], topological insulators [40], etc. RKKY exchange interaction has also been proposed to determine the magnetic ordering in spin glasses [41] and alloys [42] and to probe topological phase in silicene [43], edge states of graphene nanoribbon [44] and 2D topological insulators [45], decoupled edge modes in phosphorene [46], order of tilting in the spectrum of borophene [47] and the Fermi arc in WSM thin films [48], etc. Several experimental methods like single-atomic magnetometry and magnetotransport measurement based on angle-resolved photoemission spectroscopy (ARPES) are used to capture this exchange interaction [49–51].

The remainder of this paper in organized as follows. In Sec. II, we briefly revisit the appearance of ICM in graphene due to the IS breaking mass term across the interface. In

————
*ganeshpaul@iopb.res.in
†firoz.seikh@aalto.fi
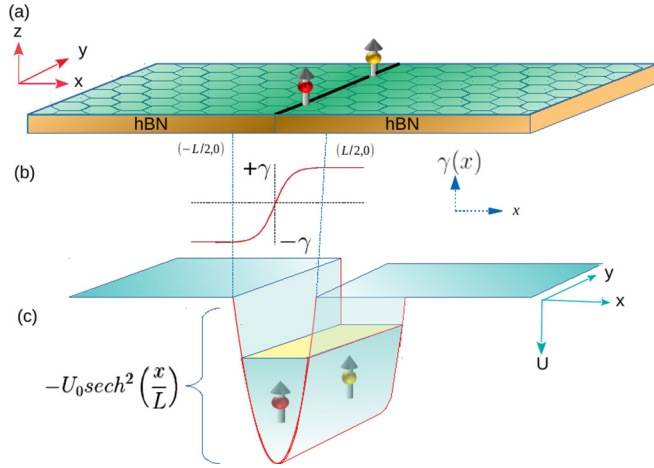‡paramita.dutta@physics.uu.se
§arijit@iopb.res.in

FIG. 1. (a) A schematic sketch of graphene, placed on the top of a hBN substrate, is depicted. The two magnetic impurities are placed on the DW which is denoted by the black solid line. (b) The smooth variation of the mass term, modeled by $\gamma(x) = \gamma \tanh(x/L)$, is shown. (c) QW of width L and height U_0, defined by the hyperbolic function, developed across the DW is symbolically illustrated.

Sec. III, we discuss the emergence of ICM due to oppositely signed momentum shifts in inversely broken WSM. The stability of both massless and massive interfacial modes against the deformation of a QW is shown in Sec. IV. Section V is devoted to the discussion of signatures of these ICM via RKKY exchange interaction (spin response). Finally, we summarize and conclude in Sec. VI.

II. MODEL AND ICM IN 2D GRAPHENE

We begin by revisiting a gapped graphene Hamiltonian [6] $H_{2D} = \boldsymbol{\sigma} \cdot \boldsymbol{k} + \gamma(x)\sigma_z$, with $\sigma \equiv \{\sigma_x, \sigma_y\}$ where σ_i's ($i \in \{x, y, z\}$) are Pauli matrices in the sublattice space and $k \equiv \{k_x, k_y\}$ is the 2D momentum operator. The mass term $\gamma(x)$ is responsible for breaking IS, which can be practically realized by placing the monolayer graphene on the top of a hexagonal boron-nitride (hBN) substrate [52,53] as depicted in Fig. 1(a). We model the mass term as $\gamma(x) = \gamma \tanh(x/L)$ so that it smoothly changes its sign across a region, namely, DW of width L around $x = 0$, shown in Fig. 1(b). The DW separating the two regions of oppositely signed mass terms is marked by a black solid line in Fig. 1(a). Consideration of the smoothly varying mass term is well justified as it is a formidable task to design a sharp boundary in reality. After decoupling the square of the eigenvalue equation, $H_{2D}\Psi = E\Psi$, we obtain

$$\left[-\frac{\partial^2}{\partial(x/L)^2} + U\left(\frac{x}{L}\right) \right]\psi_i = L^2\left(E^2 - k_y^2 - \gamma^2\right)\psi_i, \quad (1)$$

where $i \in \{A, B\}$ is the sublattice index. It resembles a 1D Schrödinger equation for the well-known Pöschl-Teller QW of width L as [54,55]

$$U\left(\frac{x}{L}\right) = -\gamma L(\gamma L + 1)\mathrm{sech}^2\left(\frac{x}{L}\right), \quad (2)$$

schematically shown in Fig. 1(c). The QW effectively describes the DW with the bound state energy given as [56]

$$E_{n=0} = \mathrm{sgn}(\gamma)k_y, \quad (3a)$$

$$E_{n>0} = \pm\sqrt{k_y^2 + 2|n|\frac{\gamma}{L} - \frac{n^2}{L^2}}. \quad (3b)$$

Note that $\mathrm{sgn}(\gamma)$ denotes the chirality of the *zeroth interfacial bound states* and the massive mode solutions are valid for $2\gamma L > |n|$. The normalized wave function is given by [56,57] $\psi_{n,k_y}(\mathbf{r}) = [e^{ik_y y}/\sqrt{L_y}]\phi_n(x/L)$ with

$$\phi_n(x) = \frac{A_n}{[\cosh(x)]^b}P_n^{b,b}[\tanh(x)], \quad (4)$$

where $P_n^{b,b}(x)$ is the Jacobi polynomial with $b = \gamma L - n$. The normalization factor is given by

$$A_n = \sqrt{\frac{n!b}{2^{2b}}\frac{(2b + |n|)!}{(\gamma L!)^2}}, \quad (5)$$

with $n_{\max} < \gamma L$. Note that the chiralities of the *zeroth interfacial bound states*, i.e., $E_{n=0}$ [Eq. 3(a)] at the two valleys are opposite to each other. Even though IS symmetry breaking does not lead to the topological phase transition, the opposite chirality is still topologically preserved as the difference of left and right moving chiral modes must be equal to the difference of the Chern numbers between left and right regions separated by the DW [2,7]. Alternatively, one can break the TRS in the two regions of the graphene where only a unidirectional ICM emerges at the two valleys [1,2,7] and thus RKKY exchange can arise nonlocally along the other edge or surface in a finite system [58]. In our case, these gapless ICM appear due to the sign change of the mass term across the boundary. They are topologically protected by the TRS present in the system and thus insensitive to how smooth sign change is (even valid for abrupt change) and also other details of the QW. However, this topological protection is absent for $n > 0$ modes being sensitive to the dimension (L) and the smoothness of the QW as clearly seen from [Eq. 3(b)]. We note that these $n > 0$ modes are similar to the Volkov and Pankratov states [59] that arise at the interface between two semiconductors or insulators with inverted mass terms [60–62].

III. ICM IN 3D WEYL SEMIMETAL

Here, we explore the appearance of ICM in IS broken 3D WSM. The IS broken WSM hosts four inequivalent Weyl nodes in the momentum space. The interfacial modes in a 3D topological hetereojunction have been considered previously with an inverted mass term [60,61] which changes sign across the interface and opens mass gaps on the both sides of the interface, i.e., a junction is made between two insulating phases. The ICM for electromagnetic waves has also been predicted in a TRS broken WSM [63]. However, in this work we consider an interface between two IS broken WSMs with oppositely signed momentum shifts instead of mass. Note that the momentum shift does not open any gap, unlike the previous studies [60,61], and hence the topological character of the Weyl nodes still persists. The low energy

effective Hamiltonian for one of these Weyl nodes reads as [64]

$$H_{3D} = k_x \tau_x + (k_y - k_0)\tau_y + [k_z - \beta(x)]\tau_z, \qquad (6)$$

where k_i's are the momentum operators, k_0 is the system parameter, and τ_i's are the Pauli matrices acting on the spin basis with $i \in \{x, y, z\}$. Here, $\beta(x)$ is the IS breaking term and, unlike graphene, it does not open any gap but shifts the Weyl nodes along the k_z direction, which is evident from the energy dispersion as $\epsilon_k = \sqrt{k_x^2 + (k_y - k_0)^2 + (k_z - \beta)^2}$. The gapless Weyl nodes are topologically protected even after the IS or TRS symmetry breaking perturbation, provided translational symmetry is preserved. Following the same prescription as in graphene, we consider the IS breaking term as $\beta(x) = \beta \tanh(x/L)$ which smoothly changes its sign across the interface. After squaring the eigenvalue equation, $H_{3D}\Psi = E\Psi$, we arrive at

$$\left[-\frac{\partial^2}{\partial x^2} + (\beta(x) - k_z)^2 - \tau_y \frac{\partial \beta(x)}{\partial x}\right]\Psi = [E^2 - (k_y - k_0)^2]\Psi. \qquad (7)$$

It can be decoupled as

$$\left[-\frac{\partial^2}{\partial (x/L)^2} + V\left(\frac{x}{L}\right)\right]\psi_j$$
$$= L^2[E^2 - \beta^2 - k_z^2 - (k_y - k_0)^2]\psi_j, \qquad (8)$$

where j denotes spin index and

$$V\left(\frac{x}{L}\right) = -\beta L(\beta L + 1)\mathrm{sech}^2\left(\frac{x}{L}\right) + 2k_z\beta L^2 \tanh\left(\frac{x}{L}\right). \qquad (9)$$

This is the well-known Rosen-Morse potential [65,66] which exhibits a minimum for $|2k_z L| < (\beta L + 1)$, indicating a region of k_z favoring the QW rather than the potential barrier. Note that the first term is exactly similar to Eq. (2) with β replaced by γ. By drawing the analogy with the Rosen-Morse QW solution, we obtain the bound state solutions with the energy eigenvalues as

$$E_{n=0} = \mathrm{sgn}(\beta)(k_y - k_0), \qquad (10a)$$

$$E_{n>0} = \pm\sqrt{\left(\frac{2n\beta}{L} - \frac{n^2}{L^2}\right)\left[1 - \left(\frac{k_z L}{\beta L - n}\right)^2\right] + (k_y - k_0)^2}, \qquad (10b)$$

where the *zeroth* solution yields the ICM ($E_{n=0}$) and the other solutions represent the massive modes ($E_{n>0}$) in WSM. This is one of the main results of our paper. The corresponding eigenstates are given by $\psi_{n,k_y,k_z}(\mathbf{r}) = [e^{i(k_y y + k_z z)}/\sqrt{L_y L_z}]\tilde{\phi}_n(x/L)$ with

$$\tilde{\phi}_n(x) = A_n \frac{e^{-ax}}{[\cosh(x)]^b} P_n^{b-a,b+a}[\tanh(x)], \qquad (11)$$

where $b \pm a = \sqrt{(\beta \pm k_z)^2 + (k_y - k_0)^2 - E_n^2}$. This reduces to $b = \beta$ and $a = k_z$ for the *zeroth* ICM. The normalization factor is given as follows:

$$A_n = \sqrt{\frac{n!}{2^{2b}} \frac{(2b+n)!}{[(b+a+n)!(b-a+n)!]} \frac{b^2 - a^2}{b}}, \qquad (12)$$

with $n_{\max} < \beta L - L\sqrt{\beta k_z}$. Interestingly, the above band structure boils down to that of graphene [see Eq. (3)] or, in

other words, the bound state solutions for the Rosen-Morse QW reduce to the Pöschl-Teller QW solutions for $k_z = 0$. Note that the zeroth ICM are immune to the details of interface and can be obtained directly from the abrupt interface, as discussed later. One can also find solutions for the other three Weyl nodes in a similar way.

IV. STABILITY OF ICM

Now, we discuss the stability of the ICM against the deformation and abruptness of the QW. So far, our results are based on a smooth QW for both graphene and WSM. In reality, the QW may not be ideally described by the hyperbolic function because of the weak deformation which might arise from the asymmetry in the smoothness of the IS breaking term on both sides of the interface. Such weak deformation can be taken into account by considering q-deformed hyperbolic functions, introduced by Arai [67] as $\sinh_q(x) = (e^x - qe^{-x})/2$ and $\cosh_q(x) = (e^x + qe^{-x})/2$ with $0 < q < 1$. This follows $q\,\mathrm{sech}_q^2(x) + \tanh_q^2(x) = 1$, $\cosh_q^2(x) - \sinh_q^2(x) = q$, and $\frac{d}{dx}\tanh_q(x) = q\,\mathrm{sech}_q^2(x)$. Hence, we model our inversion breaking term by a q-deformed hyperbolic function as $\gamma(x) = \gamma \tanh_q(x/L)$ which yields the q-deformed Rosen-Morse potential given as

$$V_q(x) = -q\beta L(\beta L + 1)\mathrm{sech}_q^2(x) + 2k_z \beta L^2 \tanh_q(x). \qquad (13)$$

Interestingly, noting the analogy with the solutions of the q-deformed Rosen-Morse potential [68], we find that the energy spectrum does not depend on q. Hence, we confirm that not only the massless ICM but even the massive modes are robust to such deformation of the QW. This robustness of the ICM elevates the potential for application and thus highly enhances the importance of the present work. Similarly to the Rosen-Morse QW for WSM, the deformed Pöschl-Teller QW corresponding to the gapped graphene also yields bound state solutions that do not depend on the degree of deformation [69]. Therefore, ICM in both graphene and WSM are robust to such deformation of the QW.

Furthermore, we show that the *zeroth* ($E_{n=0}$) ICM can be even directly obtained by considering an abrupt interface. We model the abrupt interface as $\beta(x) = -\beta[2\Theta(x) - 1]$, where $\Theta(x)$ is a Heaviside step function. The eigenvalue equation can be decoupled to write

$$\left[-\frac{\partial^2}{\partial x^2} - 2\beta\delta(x)\right]\psi_j = [(k_y - k_0)^2 + (k_z - \beta(x))^2 - E^2]\psi_j, \qquad (14)$$

which is a 1D delta-function QW problem. By employing the appropriate boundary condition across the interface at $x = 0$, we obtain an equation to determine the energy dispersion as

$$\sum_{\eta=\pm}\sqrt{(k_y - k_0)^2 + (k_z + \eta\beta)^2 - E^2} = 2\beta, \qquad (15)$$

satisfying the interfacial bound states $E = \mathrm{sgn}(\beta)(k_y - k_0)$, which is exactly the same as Eq. 10(a).

The wave functions corresponding to the ICM are $\Psi_+ \propto \exp(-x/l_+)$ for $x > 0$ and $\Psi_- \propto \exp(x/l_-)$ for $x < 0$, where $l_\pm = |k_z \pm \beta|^{-1}$ are the localization lengths of the ICM, which is not symmetric with respect to the interface. Here we quickly

comment that in graphene, the localization length is $|\gamma|^{-1}$ and thus is symmetric about the interface.

Note that the IS breaking WSM Hamiltonian is considered in real spin space, hence it is interesting to examine how the spin configuration responds to the sign changes of the momentum shift across the interface. Using the eigenstates for the ICM across the interface, we find the spin polarization for three components as $\Psi^\dagger \tau_x \Psi = 0$, $\Psi^\dagger \tau_y \Psi = \text{sgn}[E_0 + (k_z - \beta \, \text{sgn}(x))]$ and $\Psi^\dagger \tau_z \Psi \propto [1 - \text{sgn}(x)]$, which indicate that the spin polarization across the interface exhibits a sharp discontinuity along the direction of the momentum shift. For graphene, we can immediately conclude that the pseudospin polarization possesses similar discontinuity.

V. SIGNATURES OF ICM IN RKKY EXCHANGE INTERACTION

To investigate the signature of ICM via a response function in graphene and WSM, here we evaluate the RKKY exchange interaction between two magnetic impurities, mediated by the bound states of the QW. Numerous works on the RKKY exchange interaction have been carried out so far concerning Dirac materials [33–39,43,70,71], where exchange interaction takes place via bulk conduction electrons and bound states, formed inside a circular QW in graphene [72]. It is noteworthy to mention here that the RKKY exchange interaction via the bound states of a QW formed in a metallic heterostructure was considered by several groups in the early 1990s [73,74]. However, the study is still lacking as far as the signature of ICM in graphene and WSM are concerned.

For our computation, we employ the formalism (based on first quantized language) already developed in Refs. [73,74] for QWs, and very recently used in the case of graphene [72]. The total Hamiltonian in the presence of two magnetic impurities can be written as

$$\mathcal{H} = H_{2D(3D)} + \Lambda \sum_i \mathbf{s}(\mathbf{r}_i) \cdot \mathbf{S}_i, \tag{16}$$

where $\mathbf{s}(\mathbf{r}_i)$ is the spin of the conduction electrons at position $\mathbf{r}_i$ and $\mathbf{S}_i$ is the spin of the magnetic impurity. The first part of the Hamiltonian represents the Hamiltonian of the 2D or 3D system under consideration and the second term corresponds to the direct exchange interaction of the conduction electrons, of strength Λ, with the magnetic impurities. In the perturbative limit of Λ, the second-order contribution to the ground-state energy can be obtained as [74]

$$\Delta E = -\left(\frac{\Lambda}{n_c}\right)^2 \sum_{i,j} J_{\text{ex}}(\mathbf{r}_i, \mathbf{r}_j) \mathbf{S_i} \cdot \mathbf{S_j}, \tag{17}$$

where $(\Lambda/n_c)^2 J_{\text{ex}}(\mathbf{r}_i, \mathbf{r}_j)$ is the RKKY exchange interaction between the impurity spins i and j located at positions $\mathbf{r}_i$ and $\mathbf{r}_j$ respectively, and n_c is the conduction electron density. The RKKY interaction strength can be expressed in terms of the wave functions of the unperturbed Hamiltonian as [73]

$$J_{\text{ex}}(\mathbf{r}_i, \mathbf{r}_j) = \frac{1}{2} \sum_{\substack{E_\xi > \mu \\ E_{\xi'} < \mu}} \frac{\psi_{\xi'}^*(\mathbf{r_i}) \psi_\xi(\mathbf{r_i}) \psi_\xi^*(\mathbf{r_j}) \psi_{\xi'}(\mathbf{r_j}) + \text{H.c.}}{E_\xi - E_{\xi'}}, \tag{18}$$
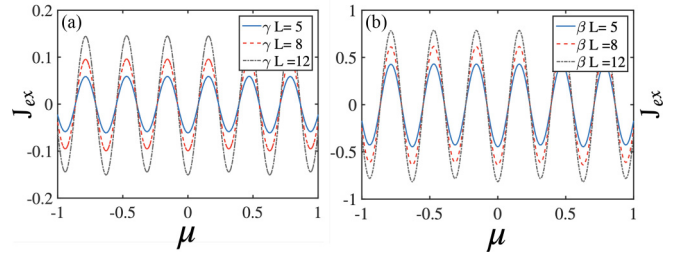

FIG. 2. J_{ex} is depicted as a function of μ for (a) graphene and (b) WSM with $x = 0$ and $y = 10L$. Here, μ and J_{ex} are normalized by γ and γL^2 (graphene) or βL^2 (WSM), respectively.

where, in the wave function $\xi = n, k_y$ (n, k_y, k_z) for 2D (3D) and μ is the chemical potential. Although ideally one should take summation over all the energy states inside as well as outside of the QW, we restrict ourselves only to the states inside the QW as we aim to extract the signature of gapless ICM close to the undoped situation.

Note that our calculation is valid in the perturbative limit of Λ [see Eq. (17)] where the second-order contribution to the ground-state energy contains the information of RKKY exchange interaction between the impurity spins which break the translational symmetry only locally. Hence, only electrons within a limited wavelength range near the Fermi energy are scattered, resulting in a density modulation around the impurity. Therefore, the band structure of graphene as well as WSM will not be significantly modified by such density oscillations in the presence of the impurities. Also, they cannot influence the topological character of the bulk as well as ICM in 2D graphene and 3D WSM.

In Fig. 2(a) we show that the RKKY exchange interaction strength for 2D graphene as a function of the chemical potential μ for three different values of the parameter γL. We restrict μ to be within the energy window where only gapless ICM appear. We find that the exchange interaction exhibits an oscillatory nature which is immune to the values of γL. This oscillatory nature is quite usual where RKKY interaction is mediated by the bulk states [33,36]. Though the *zeroth* energy ($E_{n=0}$) contribution does not depend on γL, the exchange interaction smoothly enhances via the probability wave function with the enhancement of the IS breaking term. Interestingly, unlike other systems, the behavior of J_{ex} with μ is nondecaying due to the linearity of the ICM. On the other hand, we have checked that contributions arising due to the massive modes ($E_{n>0}$) are significantly smaller than that of ICM ($\sim 10^{-3}$). Therefore, the RKKY exchange interaction is mainly dominated by the gapless modes, indicating direct signatures of ICM.

The contribution to the exchange interaction J_{ex} is mainly dominated by the ICM for which an analytical approximate form can be obtained as $J_{ex} \propto Ci[(k_c - \mu)y]$, where k_c is the momentum cutoff and $Ci(x)$ is the cosine integral which, for long distances, can be approximated as

$$Ci(\zeta) \simeq \frac{1}{\zeta}\left[\sin(\zeta) - \frac{\cos(\zeta)}{\zeta}\right]. \tag{19}$$

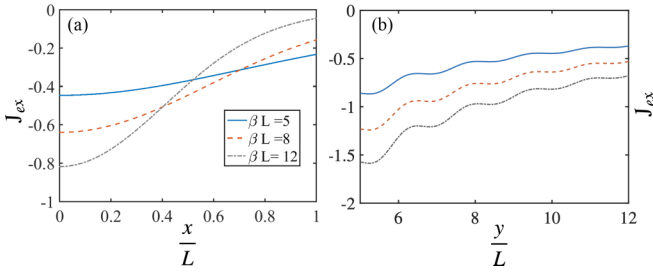Therefore, the long distance behavior is exclusively related to the linear dispersion of the ICM, which resembles the

FIG. 3. J_{ex} is demonstrated, in the case of WSM, as a function of (a) x/L and (b) y/L for various values of βL at $\mu = 0$. The normalization of J_{ex} is the same as in Fig. 2.

RKKY exchange interaction behavior along the edge modes in topological spin Hall liquid [75]. On the other hand, along the direction of QW width, the long distance limit is not desired as it is restricted by the QW width. However, a short distance limit might be further simplified by setting $\tanh(x) \simeq x$ and $\cosh(x) \simeq 1$, which yields $J_{ex} \propto [P_n^{b,b}(x)]^4$ for graphene and $J_{ex} \propto e^{-4ax}[P_n^{b-a,b+a}(x)]^4$ for WSM, indicating a relatively faster decay in the latter case.

To further reinforce our results for the signatures of the ICM in RKKY interaction, we extend our study for the 3D system, i.e., IS broken WSM, presented in Fig. 2(b). The behavior of the RKKY exchange interaction as a function of μ is oscillatory in WSM and the profile is very similar to that of graphene but with an enhanced amplitude. This enhancement of J_{ex} can be attributed to the prefactor of Eq. (12) appearing due to the third dimension of the WSM irrespective of the value of βL. Unlike graphene, the width of the QW has to be maintained quite large so that the bulk states which are gapless in either sides of the QW do not penetrate into the well. In WSM it has always been a challenging task to separate the surface modes from the bulk states as both are gapless, but in our case a segment of the surface states can only pass through the QW where bulk states are not allowed, which might be useful in probing surface modes in WSM. Note that here the *zeroth* ICM are a segment of the entire surface states which enclose the WSM.

Finally, we investigate the behavior of J_{ex} for WSM as a function of x, the distance from the center of the DW, and y, the separation between the two impurities. We present our corresponding results in Fig. 3. In Fig. 3(a), we observe that the contribution of the bound states to the exchange interaction amplitude is maximum at $x = 0$ and decays exponentially with x following the hyperbolic form of the potential of the QW. This can also be understood following the decay of the probability of the wave functions. This phenomenon is true for all βL. However, the rate of decay is much faster for higher βL. Here, we set $\mu = 0$ to consider only the $E_{n=0}$ ICM. As we increase βL, the exchange interaction increases following the envelope of $|\psi_{n=0}|^2$ and, thus, it further confirms the contributions arising solely due to ICM within the DW. In case of graphene, the RKKY interaction with "x" and "y" behaves in a very similar fashion, except for a small mismatch in decay rate which can be easily understood from the absence of the e^{-ax} term in the graphene ICM wave function.

Furthermore, when we increase the distance between the two impurities placed along the y axis, the magnitude of J_{ex}

decreases with an oscillatory envelope as shown in Fig. 3(b). This behavior of J_{ex} with the distance between the two impurities is very similar to the results for RKKY interaction via bulk states of any doped electronic system [37,39]. Also, with the enhancement of the IS breaking term, βL, there is a rise in the strength of RKKY interaction following the envelope of $|\psi_{n=0}|^2$. Note that, along both x and y directions, J_{ex} exhibits antiferromagnetic RKKY exchange ($J_{ex} < 0$) at $\mu = 0$ as the $E_{n=0}$ ICM carries two propagating modes with opposite chiralities resulting in backscattering with antiferromagnetic character.

VI. SUMMARY AND CONCLUSIONS

To summarize, in this article, we have identified the emergence of ICM in IS broken graphene (2D) and WSM (3D). We also explore the chiral bound state mediated RKKY exchange interaction between two magnetic impurities placed in them. The two magnetic impurities are localized inside a DW separating the two regions, with oppositely signed IS breaking Semenov mass terms in graphene and momentum shifting in WSM. We model the DW by a hyperbolic potential well. Most interestingly, in the undoped case ($\mu = 0$), we have found clear signatures of the ICM ($E_{n=0}$) of the gapped graphene and WSM in the RKKY exchange interaction due to their dominating contributions compared to the other bound states ($E_{n \neq 0}$) of the QW localized within the interfacial region. For any condensed matter system, it is always a challenging task to isolate surface states from the bulk states. In our case, the unique ICM are completely separated from the bulk due to the finite size of the QW engineered in both graphene and WSM.

In recent times, a few proposals have been put forwarded to extract the contributions of the Fermi arcs which appear across the interface between the WSM and vacuum via RKKY exchange interaction [48,76]. The contributions of the bulk states are inevitably present in those studies when the impurities are located at two opposite surfaces. In contrast, in our case, the RKKY exchange interaction is separated from the bulk states, bearing the contributions of only the ICM confined inside the DW.

From the practical point of view, TRS and IS broken WSM can be realized in TaAs, TaP [77,78]. Magnetic adatoms (Fe, Co, etc.) can be implanted in materials to induce magnetic moments in them [79]. An atomically precise map of the magnetic coupling between individual adatoms in pairs can be revealed in terms of spin-resolved differential conductivity following the investigation by Zhou *et al.* on the RKKY interaction by depositing Co adatoms on a Pt (111) surface [50]. They extracted the out-of-plane components of the time-averaged magnetization, both in absence and presence of an external magnetic field, to find the interaction strength. For our model, the RKKY exchange interaction strength J_{ex} can also be measured in the similar way after successfully depositing adatoms on graphene and/or WSM. The distance-dependent behavior of J_{ex} can be found by maintaining different distances between the two impurities. Spin-dependent scanning tunneling spectroscopy [50,80] can be used to measure dI/dV to identify the signature of ICM close to $\mu = 0$.

[1] F. D. M. Haldane and S. Raghu, Phys. Rev. Lett. **100**, 013904 (2008).

[2] S. Raghu and F. D. M. Haldane, Phys. Rev. A **78**, 033834 (2008).

[3] Y. Kim, K. Choi, J. Ihm, and H. Jin, Phys. Rev. B **89**, 085429 (2014).

[4] M. Ezawa, Phys. Rev. B **87**, 155415 (2013).

[5] W. Yao, D. Xiao, and Q. Niu, Phys. Rev. B **77**, 235406 (2008).

[6] G. W. Semenoff, V. Semenoff, and F. Zhou, Phys. Rev. Lett. **101**, 087204 (2008).

[7] J. Cayssol, C. R. Phys. **14**, 760 (2013).

[8] I. Martin, Y. M. Blanter, and A. F. Morpurgo, Phys. Rev. Lett. **100**, 036804 (2008).

[9] J. Jung, F. Zhang, Z. Qiao, and A. H. MacDonald, Phys. Rev. B **84**, 075418 (2011).

[10] F. Zhang, A. H. MacDonald, and E. J. Mele, Proc. Natl. Acad. Sci. USA **110**, 10546 (2013).

[11] L. Ju, Z. Shi, N. Nair, Y. Lv, C. Jin, J. Velasco, C. Ojeda-Aristizabal, H. A. Bechtel, M. C. Martin, A. Zettl, J. Analytis, and F. Wang, Nature (London) **520**, 650 (2015).

[12] A. Schroer, P. G. Silvestrov, and P. Recher, Phys. Rev. B **92**, 241404(R) (2015).

[13] H. L. Calvo, L. E. F. Foa Torres, P. M. Perez-Piskunow, C. A. Balseiro, and G. Usaj, Phys. Rev. B **91**, 241404(R) (2015).

[14] SK Firoz Islam and A. A. Zyuzin, Phys. Rev. B **100**, 165302 (2019).

[15] X. Wan, A. M. Turner, A. Vishwanath, and S. Y. Savrasov, Phys. Rev. B **83**, 205101 (2011).

[16] A. A. Burkov and L. Balents, Phys. Rev. Lett. **107**, 127205 (2011).

[17] A. A. Zyuzin, S. Wu, and A. A. Burkov, Phys. Rev. B **85**, 165110 (2012).

[18] N. P. Armitage, E. J. Mele, and A. Vishwanath, Rev. Mod. Phys. **90**, 015001 (2018).

[19] B. Q. Lv, H. M. Weng, B. B. Fu, X. P. Wang, H. Miao, J. Ma, P. Richard, X. C. Huang, L. X. Zhao, G. F. Chen, Z. Fang, X. Dai, T. Qian, and H. Ding, Phys. Rev. X **5**, 031013 (2015).

[20] Q. Chen, A. R. Kutayiah, I. Oladyshkin, M. Tokman, and A. Belyanin, Phys. Rev. B **99**, 075137 (2019).

[21] H. Nielsen and M. Ninomiya, Phys. Lett. B **105**, 219 (1981).

[22] P. Hosur, S. A. Parameswaran, and A. Vishwanath, Phys. Rev. Lett. **108**, 046602 (2012).

[23] A. A. Burkov, Phys. Rev. Lett. **113**, 247203 (2014).

[24] P. E. C. Ashby and J. P. Carbotte, Phys. Rev. B **89**, 245121 (2014).

[25] S. Jia, S.-Y. Xu, and M. Z. Hasan, Nat. Mater. **15**, 1140 (2016).

[26] Y. Baum, E. Berg, S. A. Parameswaran, and A. Stern, Phys. Rev. X **5**, 041046 (2015).

[27] G. Bednik, A. A. Zyuzin, and A. A. Burkov, Phys. Rev. B **92**, 035153 (2015).

[28] P. Dutta, F. Parhizgar, and A. M. Black-Schaffer, Phys. Rev. B **101**, 064514 (2020).

[29] Q. Chen, M. Erukhimova, M. Tokman, and A. Belyanin, Phys. Rev. B **100**, 235451 (2019).

[30] M. A. Ruderman and C. Kittel, Phys. Rev. **96**, 99 (1954).

[31] T. Kasuya, Prog. Theor. Phys. **16**, 58 (1956).

[32] K. Yosida, Phys. Rev. **106**, 893 (1957).

[33] A. M. Black-Schaffer, Phys. Rev. B **81**, 205416 (2010).

[34] E. Kogan, Phys. Rev. B **84**, 115119 (2011).

[35] P. D. Gorman, J. M. Duffy, M. S. Ferreira, and S. R. Power, Phys. Rev. B **88**, 085405 (2013).

[36] M. Sherafati and S. Satpathy, Phys. Rev. B **83**, 165425 (2011).

[37] M. Sherafati and S. Satpathy, Phys. Rev. B **84**, 125416 (2011).

[38] X. Xiao, Y. Liu, and W. Wen, J. Phys.: Condens. Matter **26**, 266001 (2014).

[39] E. H. Hwang and S. Das Sarma, Phys. Rev. Lett. **101**, 156802 (2008).

[40] J.-J. Zhu, D.-X. Yao, S.-C. Zhang, and K. Chang, Phys. Rev. Lett. **106**, 097201 (2011).

[41] P. J. T. Eggenkamp, H. J. M. Swagten, T. Story, V. I. Litvinov, C. H. W. Swüste, and W. J. M. de Jonge, Phys. Rev. B **51**, 15250 (1995).

[42] F.-s. Liu, W. A. Roshen, and J. Ruvalds, Phys. Rev. B **36**, 492 (1987).

[43] H.-J. Duan, C. Wang, S.-H. Zheng, R.-Q. Wang, D.-R. Pan, and M. Yang, Sci. Rep. **8**, 6185 (2018).

[44] J. Klinovaja and D. Loss, Phys. Rev. B **87**, 045422 (2013).

[45] C.-H. Hsu, P. Stano, J. Klinovaja, and D. Loss, Phys. Rev. B **96**, 081405(R) (2017).

[46] SK F. Islam, P. Dutta, A. M. Jayannavar, and A. Saha, Phys. Rev. B **97**, 235424 (2018).

[47] G. C. Paul, SK F. Islam, and A. Saha, Phys. Rev. B **99**, 155418 (2019).

[48] S. Verma, D. Giri, H. A. Fertig, and A. Kundu, Phys. Rev. B **101**, 085419 (2020).

[49] A. T. Hindmarch and B. J. Hickey, Phys. Rev. Lett. **91**, 116601 (2003).

[50] L. Zhou, J. Wiebe, S. Lounis, E. Vedmedenko, F. Meier, S. Blügel, P. H. Dederichs, and R. Wiesendanger, Nat. Phys. **6**, 187 (2010).

[51] A. A. Khajetoorians, J. Wiebe, B. Chilian, S. Lounis, S. Blügel, and R. Wiesendanger, Nat. Phys. **8**, 497 (2012).

[52] N. Kharche and S. K. Nayak, Nano Lett. **11**, 5274 (2011).

[53] K. Novoselov, Nat. Mater. **6**, 720 (2007).

[54] J. Lekner, Am. J. Phys. **75**, 1151 (2007).

[55] J. Diaz, J. Negro, L. Nieto, and O. Rosas-Ortiz, J. Phys. A: Math. Gen. **32**, 8447 (1999).

[56] L. D. Landau and E. M. Lifshitz, *Quantum Mechanics: Non-Relativistic Theory* (Elsevier, Amsterdam, 2013), Vol. 3.

[57] F. Freitas, arXiv:1802.06617.

[58] S. Verma and A. Kundu, Phys. Rev. B **99**, 121409(R) (2019).

[59] B. A. Volkov and O. A. Pankratov, Pis'ma Zh. Eksp. Teor. Fiz. **42**, 145 (1985) [JETP Lett. **42**, 178 (1985)].

[60] S. Tchoumakov, V. Jouffrey, A. Inhofer, E. Bocquillon, B. Plaçais, D. Carpentier, and M. O. Goerbig, Phys. Rev. B **96**, 201302(R) (2017).

[61] D. K. Mukherjee, D. Carpentier, and M. O. Goerbig, Phys. Rev. B **100**, 195412 (2019).

[62] T. L. van den Berg, A. De Martino, M. R. Calvo, and D. Bercioux, Phys. Rev. Res. **2**, 023373 (2020).

[63] A. A. Zyuzin and V. A. Zyuzin, Phys. Rev. B **92**, 115310 (2015).

[64] S.-B. Zhang, J. Erdmenger, and B. Trauzettel, Phys. Rev. Lett. **121**, 226604 (2018).

[65] N. Rosen and P. M. Morse, Phys. Rev. **42**, 210 (1932).

[66] C. B. Compean and M. Kirchbach, J. Phys. A: Math. Gen. **39**, 547 (2005).

[67] A. Arai, J. Math. Anal. Appl. **158**, 63 (1991).

[68] H. Eğrifes, D. Demirhan, and F. Büyükkiliç, Phys. Scr. **60**, 195 (1999).

[69] H. Eğrifes, D. Demirhan, and F. Büyükkılıç, Phys. Lett. A **275**, 229 (2000).

[70] H.-R. Chang, J. Zhou, S.-X. Wang, W.-Y. Shan, and D. Xiao, Phys. Rev. B **92**, 241103(R) (2015).

[71] G.-D. Wang and A.-M. Wang, Phys. Lett. A **384**, 126327 (2020).

[72] A. U. Canbolat and O. Çakır, Phys. Rev. B **100**, 014440 (2019).

[73] B. A. Jones and C. B. Hanna, Phys. Rev. Lett. **71**, 4253 (1993).

[74] J. Barnaś, Phys. Rev. B **52**, 10744 (1995).

[75] M. V. Hosseini, Z. Karimi, and J. Davoodi, J. Phys.: Condens. Matter **33**, 085801 (2020).

[76] H.-J. Duan, S.-H. Zheng, P.-H. Fu, R.-Q. Wang, J.-F. Liu, G.-H. Wang, and M. Yang, New J. Phys. **20**, 103008 (2018).

[77] S.-Y. Xu, I. Belopolski, N. Alidoust, M. Neupane, C. Zhang, R. Sankar, S.-M. Huang, C.-C. Lee, G. Chang, B. Wang, G. Bian, H. Zheng, D. S. Sanchez, F. Chou, H. Lin, S. Jia, and M. Z. Hasan, Science **349**, 613 (2015).

[78] S.-Y. Xu, I. Belopolski, D. S. Sanchez, C. Guo, G. Chang, C. Zhang, G. Bian, Z. Yuan, H. Lu, Y. Feng, T.-R. Chang, P.-P. Shibayev, M.-L. Prokopovych, N. Alidoust, H. Zheng, C.-C. Lee, S.-M. Huang, R. Sankar, F. Chou, C.-H. Hsu, H.-T. Jeng, A. Bansil, T. Neupert, V.-N. Strocov, H. Lin, S. Jia, and M. Z. Hasan, Sci. Adv. **1**, e1501092 (2015).

[79] R. Sielemann, Y. Kobayashi, Y. Yoshida, H. P. Gunnlaugsson, and G. Weyer, Phys. Rev. Lett. **101**, 137206 (2008).

[80] F. Meier, L. Zhou, J. Wiebe, and R. Wiesendanger, Science **320**, 82 (2008).